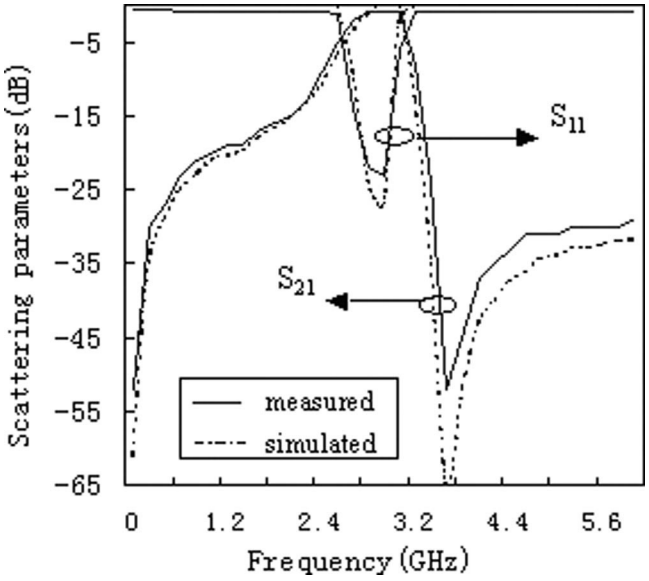

Figure 5 EM simulated and measured frequency responses of the LTCC filter with one transmission zero located at higher stopband: (——) measured; (– – –) simulated

indicates that the good agreement between the predicted and measured results is observed. The small discrepancies between the two sets of data are mainly due to fabrication error and the finite thickness of the embedded conductors that has not been included in the electromagnetic simulation.

The return loss over the passband bandwidth is better than 18 dB. The structure reveals <1.2 dB loss in the passband. This kind of filter can be used in a wireless transceiver system as a harmonic suppression filter or a part of a duplexer.

5. CONCLUSION

In this paper, a method of using admittance inverters with standard filter synthesis technique to design modified BPF with controllable transmission zeros in stopband is described. Using the proposed design approach, a novel compact LTCC filter with one transmission zero located at higher stopband is demonstrated. It is shown by simulation and measurement that this type of filter has the advantages of compact size and good performance, which allows a higher integration leading to a further wireless module miniaturization.

ACKNOWLEDGMENT

This work was supported by the Key Project of Chinese Ministry of Education (No. 104166) and by the CRT Program of UESTC.

REFERENCES

1. C.Q. Scrantom and J.C. Lawson, LTCC technology: Where we are and where we're going—II, IEEE Int Microwave Symp Dig (1998), 193–200.
2. R. Hurley and G. Sloan, An L-band, LTCC frequency doubler using embedded lumped element filters, In IEEE MTT-S International Microwave Symposium Workshop, Seattle, WA, 2002, pp. 1549–1552.
3. B.G. Choi, M.G. Stubbs, and C.S. Park, A Ka-band narrow bandpass filter using LTCC technology, IEEE Microwave Wireless Compon Lett 13 (2003), 388–389.
4. J.S. Lim and D.C. Park, A modified Chebyshev bandpass filter with attenuation poles in the stopband, IEEE Trans Microwave Theory Tech 45 (1997), 898–904.
5. G.L. Matthaei, L. Young, and E.M.T. Jones, Microwave filter, impedance-matching networks, and coupling structures, McGraw-Hill, New York, 1964. Chapter 8.
6. B.C. Wadell, Transmission line design handbook, Artech House, Boston, MA, 1991. pp. 399–402.
7. C. Hoer and C. Love, Exact inductance equations for rectangular conductors with applications to more complicated geometries, J Res Nat Bur Stand C Eng Instrum 69 (1965), 127–137.

COPLANAR WAVEGUIDE-FED BAND-SELECTIVE FILTER FOR WIDEBAND ANTENNA

Chien-Jen Wang[1] and Jin-Wei Wu[2]
[1]Department of Electronic Engineering
National University of Tainan
Tainan, Taiwan
[2]Department of Communication Engineering
National Chiao Tung University
Hsinchu, Taiwan

Received 17 April 2006

ABSTRACT: *In this study, a coplanar waveguide-fed band-selective filter and a spiral slot antenna have been designed, fabricated, and integrated for the applications of multisystem integration. The antenna module was fabricated on the same plane of the substrate, so that the circuit process and the position alignment could be simplified. The passband responses of the filter ranging below 2.6 GHz and from 5.0 to 6.0 GHz cover most of the commercial wireless communication systems. Simulated results are compared with measurements performed on the antenna module.* © 2006 Wiley Periodicals, Inc. Microwave Opt Technol Lett 48: 2264–2267, 2006; Published online in Wiley InterScience (www.interscience.wiley.com). DOI 10.1002/mop.21915

Key words: *coplanar waveguide; band-selective filter; spiral slot*

1. INTRODUCTION

Wireless communication systems attract a lot of attention for the past decades in the world because of their advantages, including convenience, low cost, and easy operation. For most of commer-

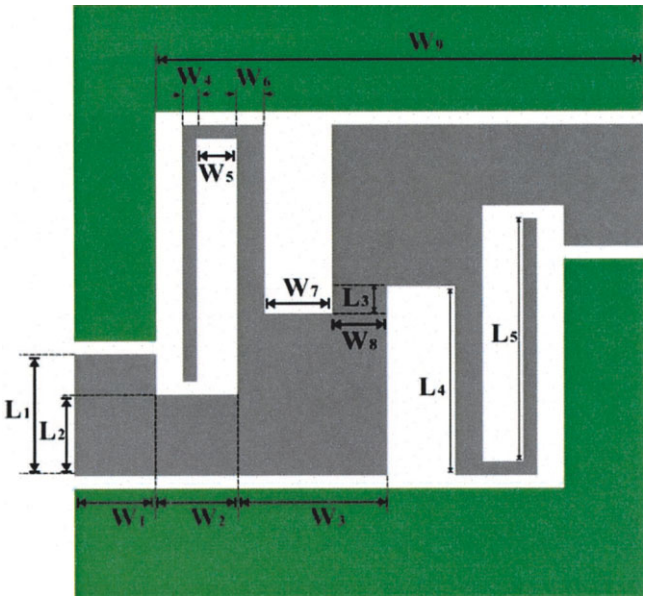

Figure 1 CPW band-selective filter. [Color figure can be viewed in the online issue, which is available at www.interscience.wiley.com]

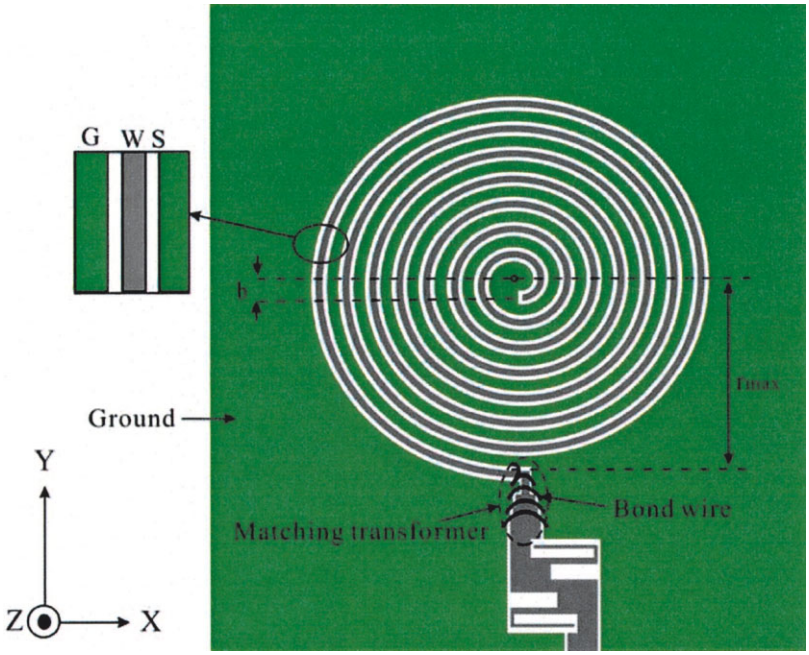

Figure 2 Schematic configuration of the band-selective antenna module. [Color figure can be viewed in the online issue, which is available at www.interscience.wiley.com]

cial wireless communication systems, such as the CDMA (825–894 MHz), GSM (890–960 MHz), GPS (1227.60 and 1575.42 MHz), DCS (1710–1880 MHz), Bluetooth (2400–2484 MHz), WLAN (2400–2483.5 MHz, 5725–5825 MHz), and HIPERLAN (5150–5350 MHz), etc., the used bandwidths distribute over below 2.65 GHz and from 5 to 6 GHz. It will be a trend for users to access multiple services and roam several networks by using a single handset or communication device. To receive the signals of the above systems and reduce the noise figure, a band-selective antenna module can be a research topic. In Ref. 1, we have demonstrated a microstrip band-selective antenna module by combining a microstrip filter and microstrip-fed spiral slot antenna, a broadband antenna. Recently, the coplanar waveguide (CPW) structure has gradually replaced the microstrip-line technology in the design of filters due to the merits such as insensitive to the substrate thickness, high circuit density, low dispersion, and radiation losses, ease in series and shunt connections, suitability to photolithographic fabrication, and no via hole, etc [2–4].

In this study, a CPW band-selective antenna module has been demonstrated. The CPW-fed wideband spiral slot antenna is integrated with the filter to achieve a band-selective bandwidth. The

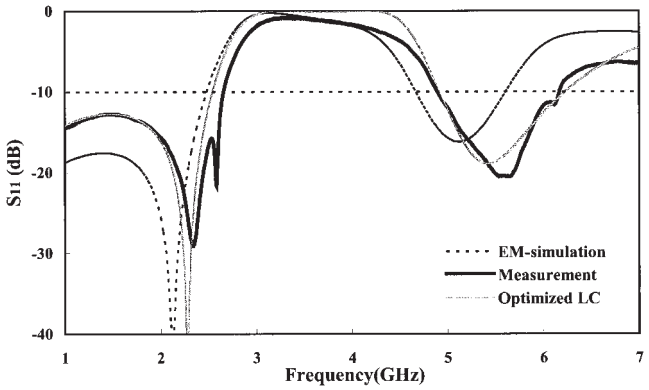

Figure 3 Comparison of the reflection coefficients of the filter

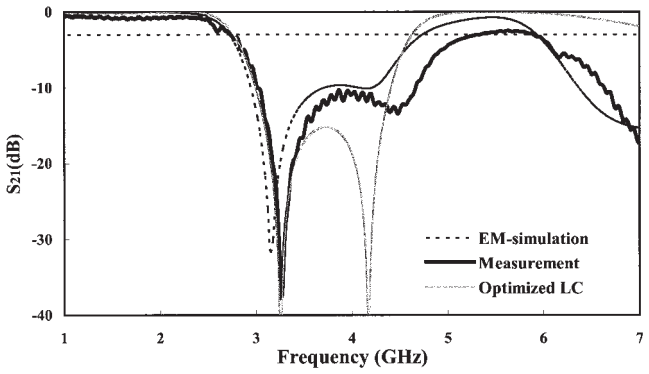

Figure 4 Comparison of the transmission coefficients of the filter

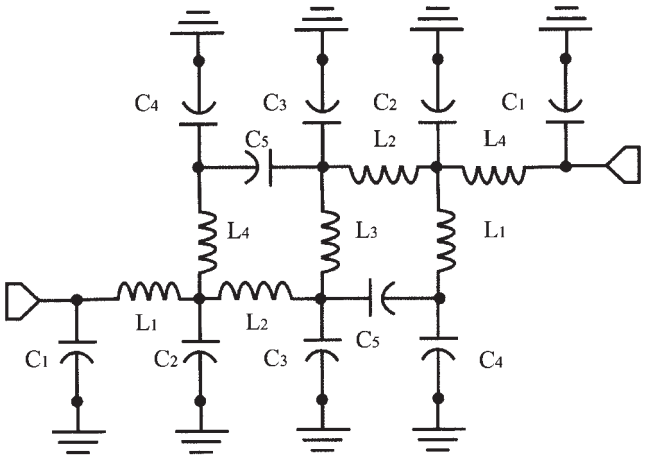

Figure 5 Lumped-element equivalent-circuit model

TABLE 1 Equivalent *L–C* Values from the Approximated *L–C* Values and Optimized *L–C* Values

	C_1	C_2	C_3	C_4	C_5	L_1	L_2	L_3	L_4
Approximated LC-values	0.20 pF	0.49 pF	0.28 pF	0.17 pF	0.25 pF	0.76 nH	0.17 nH	3.1 nH	1.5 nH
Optimized LC-values	0.50 pF	0.30 pF	0.053 pF	0.50 pF	0.21 pF	0.38 nH	0.096 nH	2.18 nH	2.04 nH

LC-equivalent model of the CPW band-selective filter is extracted and calculated. According to the measured results, the antenna module covers the specifications of the systems of GSM, GPS, DCS, PHS, CDMA, Bluetooth, WLAN, Hiper-LAN, and ITS.

2. DESIGN

Figure 1 shows the configuration of the proposed CPW filter, which is designed and fabricated on high-frequency FR-4 substrate with dielectric constant of 4.4 and substrate thickness of 1.6 mm. To reduce the filter size, two $1/4\lambda_g$ open stubs are used in the form of bent or folded stub structure [5, 6], (λ_g was the guided wavelength at 3.8 GHz, the center frequency of the forbidden band from 2.6 to 5.0 GHz). The frequency response of the filter is realized by utilizing the combination of the band-stop filter ($1/4\lambda_g$ open stubs) and the low-pass filter (the bent stepped-impedance line). It was noted that the bandwidth of the forbidden band was controlled by the characteristic impedance of the $1/4\lambda_g$ open stubs. The tested antenna module, including the broadband CPW-fed spiral slot antenna and the CPW filter, is shown in Figure 2. The feeding structure and the spiral radiator were designed on the top plane of the substrate, so that fabrication of the circuit and position alignment could be simplified. The empirical formula shown in Eq. (1) was used to determine the initial resonant frequency of the antenna.

$$\lambda_L = 2\pi r_{\max}, \tag{1}$$

where λ_L is wavelength of the initial resonant frequency Fini and $r_{\max}$ radius of the first outer slot.

A CPW matching transformer is added between the signal input and the spiral slot antenna to obtain a better impedance matching condition. It is known that a nonsymmetric CPW discontinuity of the circuit, such as a bend, excites the parasitic coupled slotline mode. This mode propagates at a different velocity from the dominant even CPW mode and causes a leakage of radiation to free space. Several air bridges were bond-wired across the feedline, so that a leakage of the surface wave could be suppressed.

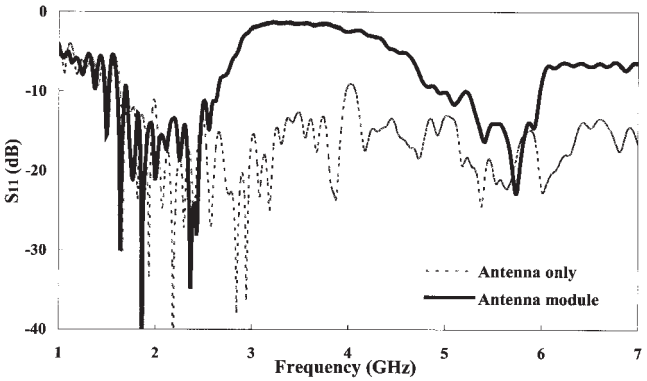

Figure 6 Comparison of the measured reflection coefficients of the antenna and module

3. RESULTS

In this study, the EM simulation tool, Ansoft Ensemble V8.0 and the high-frequency circuit-simulation software Microwave Office

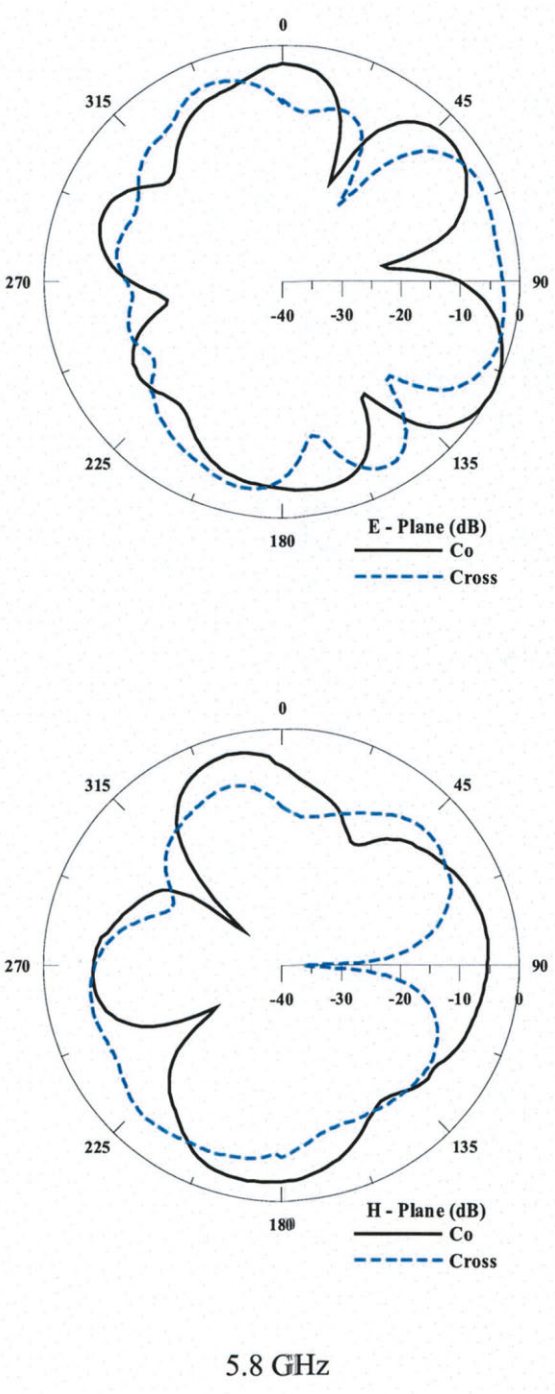

Figure 7 Measured radiation patterns of the band-selective antenna module. [Color figure can be viewed in the online issue, which is available at www.interscience.wiley.com]

2002 were utilized to calculate the S parameters of the band-selective filter. The S parameters of the proposed circuits in this study were measured by using an Agilent E8362B PNA series network analyzer. Figures 3 and 4 show a comparison of the simulated and measured S parameters of the CPW band-selective filter. The pass-band responses operated below 2.6 GHz and from 5.0 to 6.0 GHz. Figure 5 shows the LC-equivalent model of the proposed filter. The values of the lumped elements are analyzed and calculated by utilizing the transmission line model. Table 1 presents the equivalent lumped-element values from the approximate *L–C* values and optimized *L–C* values. Figure 6 shows the comparison of the measured reflection coefficients of the CPW-fed spiral slot antenna and one integrated with the CPW band-selective filter. The antenna module covers the frequency bands of the wireless communication systems and filters out the out-of-band signals, so that the received noise can be suppressed and the noise figure can be reduced. Figure 7 presents the measured radiation patterns of the *E* and *H* planes of the slot antenna at 1.8, 2.4, 5.2, and 5.8 GHz. The power intensity of the cross-polarization radiations of the CPW-fed antennas was similar to one of the copolarization radiations. This phenomenon may be attributed to the enhancement of the surface wave because of the CPW feeding structure and the spiral radiation aperture of the antenna. The irregular radiation patterns measured at 5.2 and 5.8 GHz showed that the power leakage was due to a combination of the dominant, traveling, and surface-wave modes. The measured antenna gain was about 1.75 dB at 1.8 GHz.

4. CONCLUSION

In this study, a CPW-fed band-selective filter is demonstrated for the use of the wideband spiral slot antenna. By placing the band-selective filter between the wideband antenna and low noise amplifier, the out-of-band signals are rejected such that the noise figure of the communication systems could be reduced. This design of the CPW antenna module can be useful for the monolithic microwave integrated circuit.

REFERENCES

1. C.J. Wang, C.H. Lin, and J.W. Wu, A microstrip filter utilized in ultra-wideband antennas, Microwave and Opt Technol Lett 41 (2004), 248–251.
2. F.L. Lin and R.B. Wu, Computations for radiation and surface-wave losses in coplanar waveguide bandpass filters, IEEE Trans Microwave Theory Techn 47 (1999), 385–389.
3. Y.K. Kuo, C.H. Wang, and C.H. Chen, Novel reduced-size coplanar-waveguide bandpass filters, IEEE Microwave Wireless Components Lett 11 (2001), 65–67.
4. A. Görür and Ö. Akgün, Resonance characteristics of capacitively loaded CPW open-loop resonators, Microwave Opt Technol Lett 38 (2003), 298–300.
5. J.W. Bandler, R.M. Biernacki, S.H. Chen, D.G. Swanson, Jr., and S.Ye, Microstrip filter design using direct EM field simulation, IEEE Trans Microwave Theory Tech 42 (1994), 1353–1359.
6. S.S. Liao, H.K. Chen, Y.C. Chang, and K.T. Li, Novel reduced-size coplanar waveguide bandpass filter using the new folded open stub structure, IEEE Microwave Wireless Components Lett 12 (2002), 476–478.

DISTRIBUTED HYBRID-FIBER RAMAN AMPLIFIERS WITH A SECTION OF NONLINEAR MICROSTRUCTURED OPTICAL FIBER

Yan-ge Liu, Chao Wang, Tingting Sun, Yan Li, Zhi Wang, Chunshu Zhang, Guiyun Kai, and Xiaoyi Dong
Key Laboratory of Opto-Electronic Information Science and Technology
Ministry of Education, Institute of Modern Optics
Nankai University
Tianjin 300071, China

Received 30 March 2006

ABSTRACT: *A distributed hybrid-fiber Raman amplifier with a 25-km single-mode fiber and a section of nonlinear microstructured optical fiber (NMOF) is proposed and experimentally investigated in detail. Three pump schemes and span configurations, as well as two NMOF types with different parameters and length were considered. The influence of the NMOF presence on the performance of the amplifier was analyzed.* © 2006 Wiley Periodicals, Inc. Microwave Opt Technol Lett 48: 2267–2271, 2006; Published online in Wiley InterScience (www.interscience.wiley.com). DOI 10.1002/mop.21901

Key words: *fiber Raman amplifiers; microstructured optical fiber (MOF); photonic crystal fiber (PCF)*

1. INTRODUCTION

Microstructured optical fibers (MOFs), also called photonic crystal fibers (PCFs), have attracted considerable interest in recent years due to their unique characteristics such as endlessly single-mode property [1], highly effective nonlinearity [2], and controllable dispersion property [3]. Such fibers consist of a pure silica core surrounded by a regular array of longitudinal air holes and can be designed to have effective mode area A_{eff} at least as small as 1.7 μm^2 at 1550 nm [4]. Hence, they can provide an effective nonlinearity per unit length which can be an order or more higher than that of a conventional fiber. The enhanced nonlinear properties of MOFs can be exploited for Raman amplification [5–8]. A continuous-wave pumped Raman laser [5], as well as an L^+-band Raman amplifier [6] in a PCF, have already been experimentally demon-

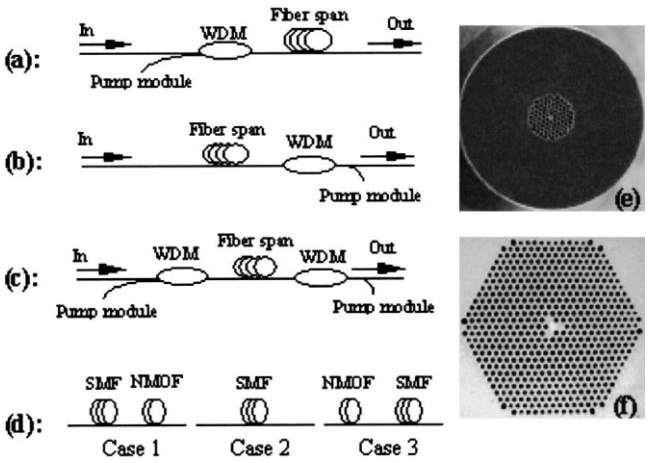

Figure 1 Experimental setup: (a) forward-pumped configuration, (b) backward-pumped configuration, (c) bidirectional-pumped configuration, (d) fiber configuration of the span, (e) and (f) is the transverse structure of NMOF1 and NMOF2